Journal of
Materials Chemistry C

Materials for optical, magnetic and electronic devices

Accepted Manuscript

This article can be cited before page numbers have been issued, to do this please use: L. Ouyang, S. Buchmann, T. Benselfelt, C. Musumeci, Z. Wang, S. Khaliliazar, W. Tian, H. Li, A. Herland and M. M. M. Hamedi, *J. Mater. Chem. C*, 2021, DOI: 10.1039/D1TC03599A.

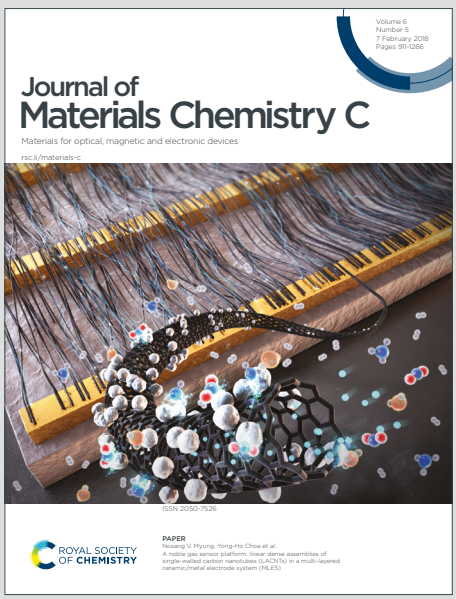

ROYAL SOCIETY OF CHEMISTRY

rsc.li/materials-c

Rapid Prototyping Heterostructured Organic Microelectronics using Wax Printing, Filtration, and Transfer

View Article Online
DOI: 10.1039/D1TC03599A

*Liangqi Ouyang[+], Sebastian Buchmann[+], Tobias Benselfelt, Chiara Musumeci, Zhen Wang, Shirin Khaliliazar, Weiqian Tian, Hailong Li, Anna Herland, Mahiar M. Hamedi**

Dr. L. Ouyang, Dr. T. Benselfelt, Dr. Z. Wang, S. Khaliliazar, Dr. W. Tian, and Prof. M. Hamedi
Fibre and Polymer Technology (FPT) School of Engineering Sciences in Chemistry, Biotechnology and Health, KTH Royal Institute of Technology, Teknikringen 56, 11428, Stockholm, Sweden
*Corresponding author, e-mail: mahiar@kth.se

S. Buchmann, Prof. A. Herland
Division of Micro- and Nanosystems (MST), KTH Royal Institute of Technology, Malvinas Väg 10, Stockholm, Sweden

Dr. C. Musumeci
Laboratory of Organic Electronics, ITN, Linkoping University, Campus Norrkoping, SE 60221, Sweden

Dr. H. Li
Fysikum, Stockhohlm University, Roslagstullsbacken 21, Stockholm Sweden

+Shared authors

Keywords: printed electronics, conducting polymers, electronic heterostructures, micropatterning, self-assembly

View Article Online
DOI: 10.1039/D1TC03599A

Abstract

Conducting polymers are the natural choice for soft electronics. The main challenge is, however, to pattern conducting polymers using simple and rapid method to manufacture advanced devices. Filtration of conducting particle dispersions through a patterned membrane is a promising method. Here we show rapid prototyping of various micropatterned organic electronic heterostructures of PEDOT:PSS by inducing the formation of microscopic hydrogels which are then filtered through membranes containing printed hydrophobic wax micropatterns. The hydrogels are retained on the un-patterned, hydrophilic regions, forming micropatterns, achieving resolutions down 100 μm. We further solve the problem of forming stacked devices by transferring the acidified PEDOT:PSS micropattern using adhesive tape transfer, to form vertical heterostructures with other micropatterned electronic colloids like CNTs, patterned using similar technique. We demonstrate a number of different heterostructured devices including micro supercapacitors and organic electrochemical transistors, and also demonstrate the use of the acidified PEDOT:PSS microstructures in cell cultures to enable bioelectronics.

1. Introduction

Organic electronic materials, especially solution-processible conducting polymers,[1] form soft, conformal, high surface area, conductive microstructures on various surfaces. One class of organic electronic material that has been used very successfully for various applications is the conducting polymer (CP) polyethylene(dioxythiophene):polystyrene sulfonate (PEDOT:PSS). PEDOT:PSS is an active material for making soft displays, actuators, and bio-interfaces with skin, cell, and brain contacts.[2] To fabricate advanced devices, however, PEDOT:PSS has to be micropatterned and/or stacked onto other patterned functional materials and substrates, such as metals and conductive carbon. The micropatterning of electronic heterostructures rely mainly on conventional microfabrication techniques in cleanroom environments, with

View Article Online
DOI: 10.1039/D1TC03599A

multiple steps involving spin coating of electronic materials combined with photolithography and etching steps.[3] This technique is time consuming, expensive, and the etching steps can be determinantal for some organic conductors. The residues of etchants and resists can also affect biocompatibility. It is furthermore difficult to perform photolithography on arbitrary substrates like flexible materials. Another technique which does not involve microfabrication is printing, e.g., inkjet[4], or screen printing[5]. For screen printing, inks with special rheological properties have to be developed for meshes. In inkjet printheads, inks of colloidal particles often clog the nozzles. More problematically, it is hard to fabricate complex geometries with multiple stacks of various materials using any additive printing methods, because the addition of inks from water can dissolve and alter the previous layers.

3D printable PEDOT:PSS inks have been developed for the patterning of complex geometries in combination with other non-conductive printable materials, but these processes rely on time-consuming mechanisms such as cryogenic freezing, lyophilization, and dry annealing.[6] To solve this problem, we[7,8] and others[9] recently developed a patterning technique where a wax printer is used to pattern hydrophilic substrates, such as PVDF filtration membranes, and aqueous dispersions of colloids are subsequently vacuum filtered through the membrane, whereupon the materials are retained on the un-patterned, hydrophilic regions to form micropatterns. This method has been employed to pattern silver nanowires,[9] gold nanowires,[10] carbon nanotubes (CNT),[11] and MXene[8] into single layer functional devices. It has however until now not been possible to pattern polymers such as PEDOT:PSS with this technique, because polymers and polymer dispersions pass through the filtration membranes. Furthermore, this technique has not enabled the fabrication of stacked structures of different conductors and electrolytes which are necessary for advanced devices.

Here we developed acidified PEDOT:PSS (a-PEDOT:PSS) microgels. These microgels could be retained on a wax-patterned membrane to form distinct micropatterns with resolution down to 100 μm. In contrast to previously reported patterned electrode arrays using a-PEDOT:PPS,

View Article Online
DOI: 10.1039/D1TC03599A

the method described here does not rely on photolithography or wet etching processes and can be patterned on flexible substrates.[12] We also post-treat the micropatterned structures with methanol to form highly water-resistant conducting a-PEDOT:PSS electrodes. We further solve the problem of forming stacked devices by transferring the a-PEDOT:PSS micropattern through tape peeling, to form vertical heterostructures with other micropatterned electronic colloids, such as CNTs. We demonstrate a number of different devices and finally we show that these a-PEDOT:PSS microstructures can be used in cell cultures to enable bioelectronics.

2. Result and Discussion

2.1. PEDOT microgels

PEDOT:PSS is one of the most widely used organic electronic materials thanks to its high conductivity and stability.[13] Through the tuning of doping level and morphology, the conductivity of PEDOT:PSS can be varied from semiconducting to metallic.[14] As an electroactive material, PEDOT:PSS is stable both in vivo and in vitro. Commercially, high conductivity PEDOT:PSS is available as a dispersion of particles with diameters of around 20 nm.[15] This fine dispersion passes through filtration membranes.[16] To pattern PEDOT:PSS into electronic devices, in-situ gelation through crosslinking reagents,[17, 18] or pre-patterning of oxidizer layer is used.[19] On the other hand, PEDOT:PSS is a polyelectrolyte complex in which positively charged PEDOT is charge-compensated and stabilized by negatively charged PSS. Divalent cations, such as copper (II)[17] and magnesium (II)[20], can induce gel formation of PEDOT:PSS by crosslinking of PSS^-. Previously, it was found that sulfuric acid increases the doping level of PEDOT:PSS, which is accompanied by the release of a portion of free PSS from the PEDOT:PSS complex and the reorganization of PEDOT regions.[21] Here we studied this phenomenon more systematically, by using in-situ rheology measurement during the acidification of PEDOT:PSS (see experimental). **Figure 1A** shows rapid gelation with an initial locking within 2-3 minutes followed by a long term and slow consolidation which did

View Article Online
DOI: 10.1039/D1TC03599A

not reach equilibrium within the 30 minutes of the measurement. The gelation is concentration dependent because a rubbery gel is formed at 1 M sulfuric acid, whereas a viscous non-Newtonian liquid is formed at 0.1 M. Figure 1B provides further insight into this dynamic behavior and clearly shows a rubbery plateau and gel behavior in the case of 1M sulfuric acid, and a shear thickening viscous liquid for the 0.1 M case. The reference, as received, PEDOT:PSS dispersion has a behavior closer to that of a Newtonian liquid. We observed, a yield strain of 60% and 20% in the case of 0.1 and 1 M sulfuric acid, respectively. Figure 1C illustrates the gelling property. When a droplet of 1 M sulfuric acid is placed next to a droplet of PEDOT:PSS, a blue a-PEDOT:PSS gel is immediately formed at the border of the two droplets.

To fabricate suspended microgel particles, we first formed large millimeter sized blocks of aggregates (see Figure 1D) through acidification. We collected these flakes by centrifugation, which also removed the excessive acid in the supernatant. Finally, we created a-PEDOT:PSS micro-gels by vigorously stirring the collected aggregate gel dispersion in water, see schematic Figure 1F. The a-PEDOT:PSS microgels were colloidally stable in water without visible precipitation for a minimum of two weeks. The acidification and re-dispersion resulted in microgel particle sizes in the scale of several micrometers (as visible from micrographs Figure 1E, and more detailed from the AFM phase images in Figure S1) so that they could be rapidly dewatered, and retained on filtration membranes for micropatterning.

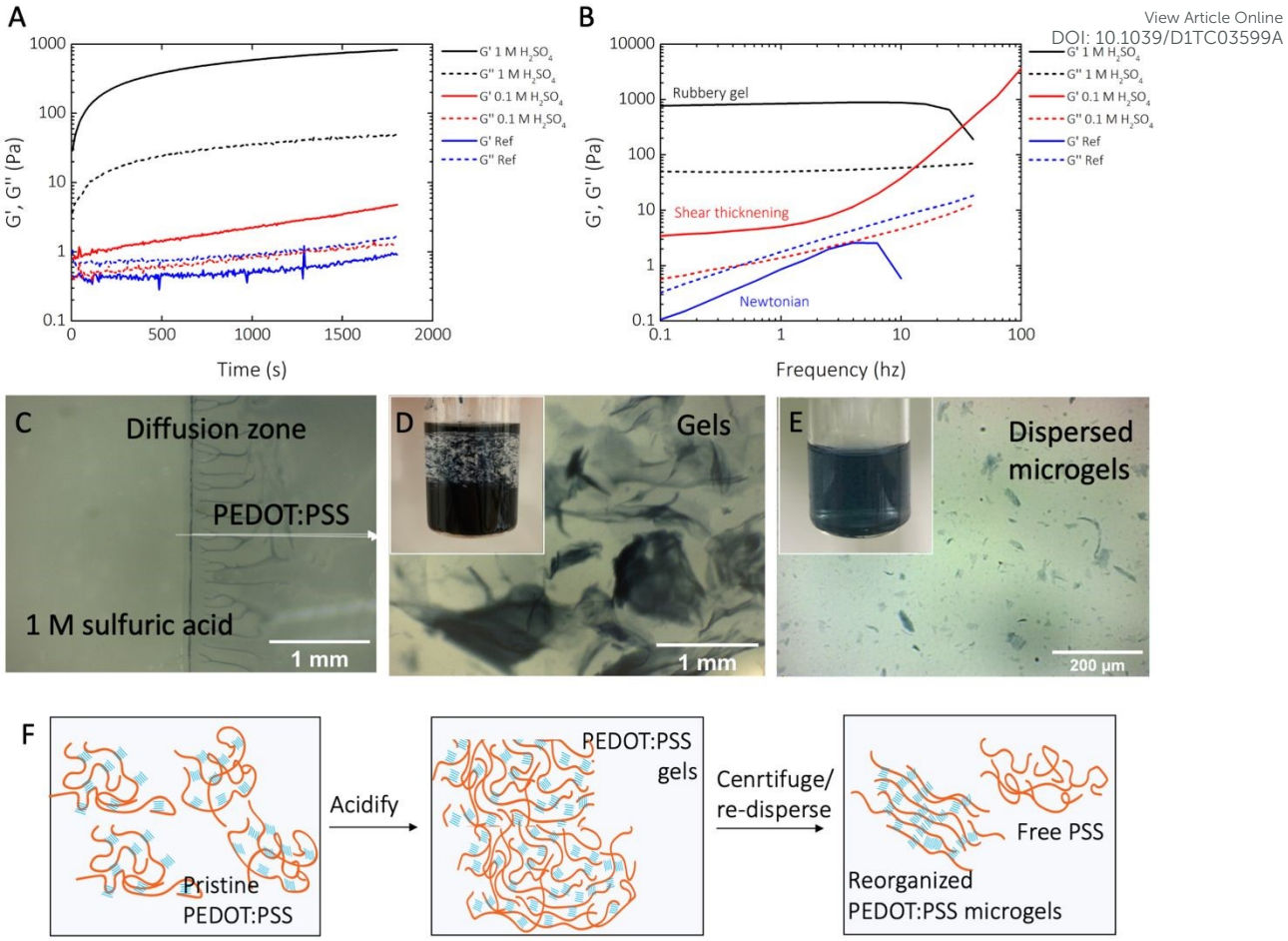

Figure 1. Acidified PEDOT:PSS for patterning.(A) Rheology data showing the storage (G') and loss modulus (G'') as function of time after gel initiation by sulfuric acid. (B) Rheology data showing the storage and loss modulus at different frequencies of the oscillator. Black and red represent PEDOT:PSS in different acid concentrations, and blue line is PEDOT:PSS in water. (C) An interface between droplets of 1 M sulfuric acid and PEDOT:PSS showing the formation of the aggregates during sulfuric acid diffusion into PEDOT:PSS, which induced gelation of PEDOT:PSS. (D) Optical micrograph showing large flakes of a-PEDOT:PSS gel. The inset is a photo of aggregated a-PEDOT:PSS flakes floating in water. (E) Optical micrograph showing re-dispersed a-PEDOT:PSS microgel. The inset is a photo of the microgels suspended in in water. (F) Schematic of proposed process during PEDOT:PSS acidification and dispersion.

View Article Online
DOI: 10.1039/D1TC03599A

2.2. Tuning the stability and conductivity with post-treatments

Many solvents, for example, dimethyl sulfoxide and diethylene glycol, induce the phase separation between PEDOT and PSS and therefore enhance the connectivity and conductivity of PEDOT:PSS.[22] We hypothesized that these treatments could also promote the interaction between PEDOT segments, creating a water-stable, crosslinked network. We chose methanol because it has a low boiling point and therefore evaporates quickly when added on top of patterned a-PEDOT:PSS.[23] AFM images showed a distinct difference in surface morphologies between a-PEDOT:PSS and methanol treated PEDOT:PSS films (Figure S1A). We formed a film using the a-PEDOT:PSS microgels and record a sheet resistance of 605 ± 76 Ω sq^{-1}. Rinsing with methanol decreased the sheet resistance of patterned structures to 232 ± 63 Ω sq^{-1} (Figure S1B). We then immersed the films into water and without methanol treatment, the a-PEDOT:PSS film quickly swelled, delaminated from the substrate, and disintegrated. Methanol treated films, however, showed superior stability in water. After 3 hours in water, the sheet resistance slightly increased to 251 ± 63 Ω sq^{-1} without any observable degradation or cracking of the films**.**

2.3. Micropatterning of a-PEDOT:PSS using printing, and characterization of basic properties

We used the a-PEDOT:PSS microgels for micropatterning electronic structures as shown schematically in **Figure 2A** and **2B**. Briefly, we used printed wax patterns onto PVDF membranes (pore size 0.45 or 0.25 μm). The versatility of the wax printing allowed us to print arbitrary shapes with precisions around 100 μm. Next, we micropatterned the aqueous dispersion of a-PEDOT:PSS microgels by filtration through the membrane. The hydrophobic wax layer repels dispersed particles, forming patterns on the hydrophilic parts of the membrane. By controlling the amount of liquid and the concentration that passes through the filter membrane per wax free area, as all a-PEDOT:PSS microgel remains in the filter, it is

View Article Online
DOI: 10.1039/D1TC03599A

possible to control the final thickness and thus the sheet resistance of the patterned a-PEDOT:PSS layer (**Figure S1B**). We subsequently transferred the patterns from the membrane by pasting and peeling with adhesive tape. These thin micropatterned a-PEDOT:PSS films were intrinsically flexible and could sustain mechanical deformations during the peeling.

To analyze the resolution of filtration-assisted micropatterning of a-PEDOT:PSS, we formed thin line shapes with various widths and gaps. As shown in Figure 2C, the minimal line resolution achievable was around 100 µm, which is due to limitations of the wax printer and not the filtration assisted patterning technique. Due to the structure of the microgels, the filtration patterned a-PEDOT:PSS showed fuzzy and rough edges. A minimal gap distance of 100 µm was, however, still achievable. Both the line and gap could be reliably patterned at a resolution of 200 µm. This resolution was in line with that reported for MXene[8] or metal nanowires[9], using the same patterning technique and is sufficiently high for a many of device fabrications for example in wearable electronics and analytical applications[24].

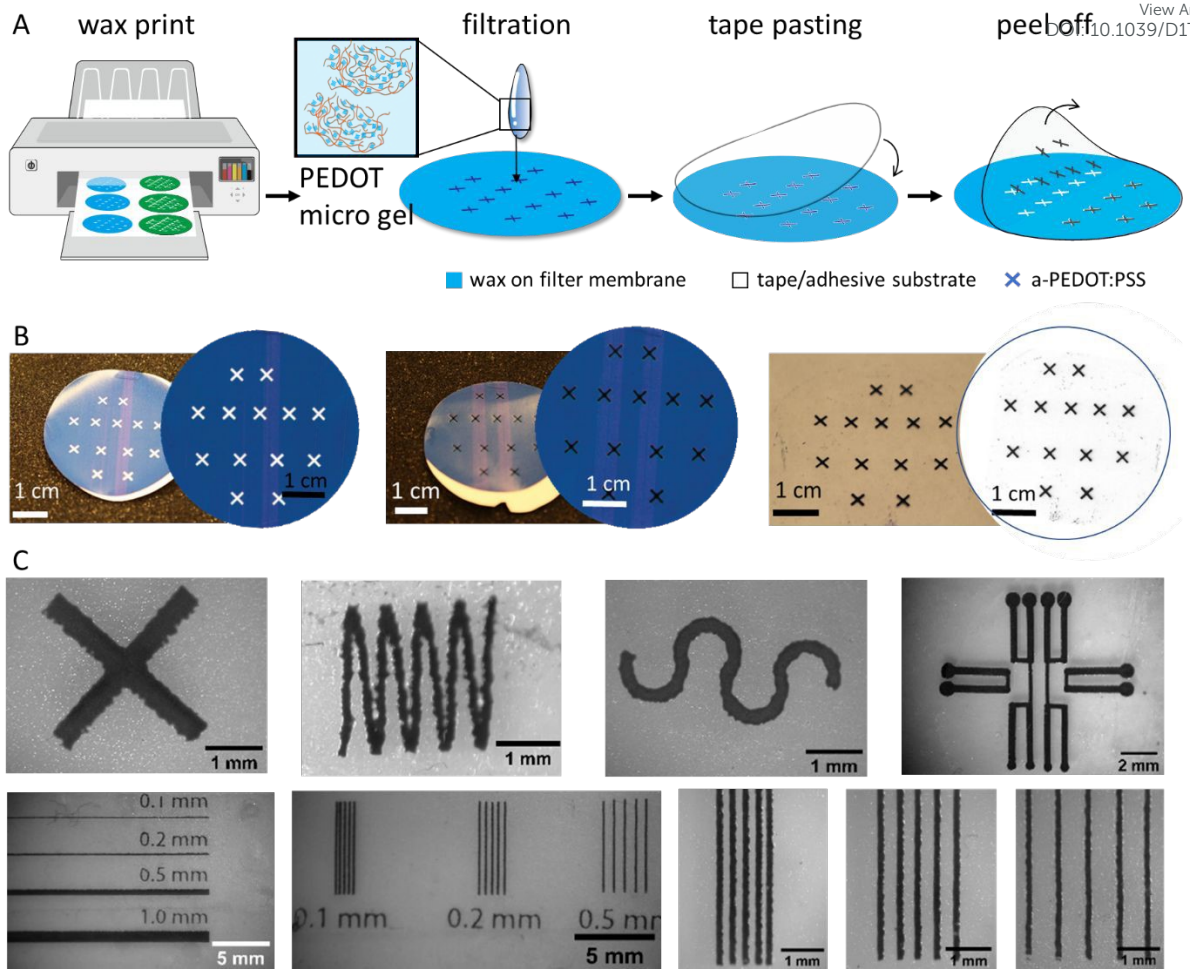

Figure 2 (A) Schematics of the filtration-assisted patterning of a-PEDOT:PSS microgel. (B) Photographs of the different stages of patterning, from left the right: 1. the wax patterned filtration membrane, 2. a-PEDOT:PSS on the membrane, and 3. a-PEDOT:PSS patterns transferred onto transparent tape. The right side of each panel is a scanned photograph. (C) Optical micrographs of representative patterned a-PEDOT:PSS: cross, zigzag and serpentine shapes, optical micrograph of arrays of a-PEDOT:PSS channels, resolution test of a-PEDOT:PSS with lines of various size with the thinnest line is 100 µm - note that the letters were also patterned in a-PEDOT:PSS – and resolution test showing the minimal gap distance between each line of 200 µm.

View Article Online
DOI: 10.1039/D1TC03599A

Additionally, the gel property of a-PEDOT:PSS allows the patterned a-PEDOT:PSS films to heal upon rewetting. (**Figure S2 and S3**).

The a-PEDOT:PSS pattern form an electrochemical active surface that is accessible to ions. To estimate its surface area, we patterned bar-bell electrodes and measured their electrochemical surface areas from CVs using Randels-Sevick equation (Figure S4). For a geometric area of 7 mm^2, we estimated an electrochemical surface area of 32 ± 2 mm^2 , suggesting that the microgel network provides significant amount of electroactive sites in its bulk.[25] This observation is also in accordance with the high surface area typically reported for PEDOT:PSS modified metal substrates.[26]

2.4. Heterostructures

With a-PEDOT:PSS as the active materials and assisted by the peel-and-transfer method, we show that the method can be used to pattern microscale devices with multilayered heterostructures. For this purpose, we also patterned single-walled CNT dispersed in water using the same method. **Figure 3A** shows the schematics of the general approach for fabrication of heterostructures: we patterned CNT electrodes and transferred these patterns from the filter membrane onto tape which was pre-patterned with a-PEDOT:PSS microstructures (as described in section 2.3) to form multilayers, as shown in Figures 3B and 3C. After methanol treatment, a-PEDOT:PSS and CNT channels formed a compact electronic contact with each other as shown in Figure 3D and 3E. We could therefore use the CNTs as electrodes to contact the a-PEDOT:PSS, this is useful in many devices including transistors. We could measure the resistance of a “cross” shaped a-PEDOT:PSS between two CNT electrodes to 1200 Ω after methanol treatment.

View Article Online
DOI: 10.1039/D1TC03599A

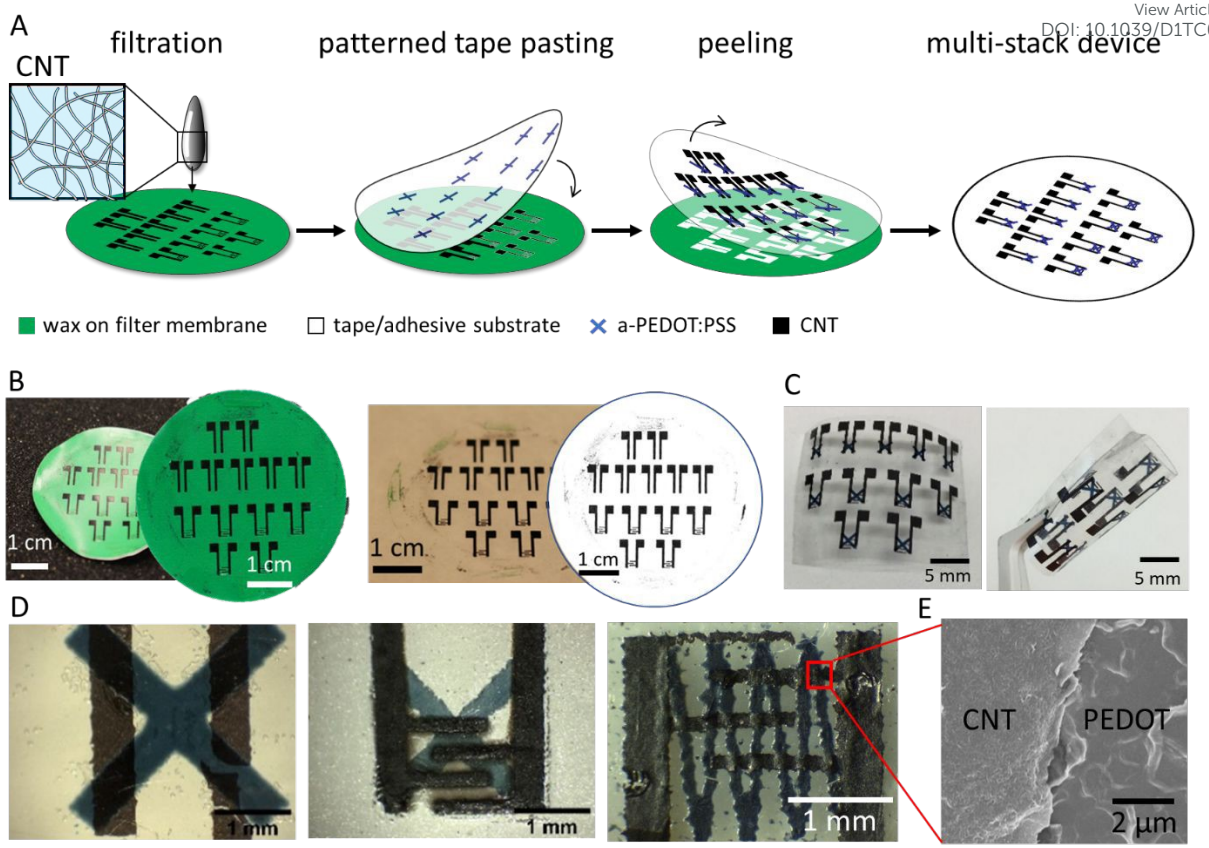

Figure 3. (A) Schematics of the filtration-assisted patterning of carbon nanotubes CNT, from dispersion, and the fabrication of multi-stack, heterogeneous devices by joining these pattern with a-PEDOT:PSS patterns. (B) Photographs of CNT patterns on wax patterned filtration membrane (left) and the CNT patterns transferred onto transparent tape (right). The right side of each panel is the scanned image from the sample. (C) Photograph of a 2-layer device with a-PEDOT:PSS and CNT micropatterns (D) Photographs of a 2-layer transistor arrays with methanol treated CNT as electrodes and a-PEDOT:PSS "cross" or "serpentine" shapes as channel on a flexible substrate. (E) SEM image of the cross section between the a-PEDOT:PSS and the CNT in a 2-layer stacked device after methanol treatment.

2.5. Micropatterned multilayer Organic electrochemical transistors (OECTs) and Supercapacitors

View Article Online
DOI: 10.1039/D1TC03599A

The patterning method allowed us to pattern interdigitated electrodes, which is a useful geometry, see schematic **Figure 4A**, for micro supercapacitors and electroanalytical micro devices, at a resolution of 200 μm without defects and shorts (Figure 4B). Higher resolution is also achievable, although increasing the risk of creating shorts when the gap between the interdigitated a-PEDOT:PSS electrodes is decreased. We casted a 1 M aqueous NaCl solution onto interdigitated methanol treated a-PEDOT:PSS electrodes as the electrolyte to create a planar micro supercapacitor. The CVs of the device at different scan rates are shown in Figure 4C, and charge/discharge curves in Figure 4D. At a scan rate of 2 mV s^{-1}, we achieved a specific capacitance of 1.6 mC cm^{-2}. We note that this number is on the lower end of PEDOT:PSS supercapacitors compared to previously reported capacitors, due to the relatively low conductivity of PEDOT:PSS itself as both an active material and the current collector.[27] To demonstrate more advanced devices, we fabricated organic electrochemical transistors (OECTs). These are based on the semiconducting, electrochemically active properties of PEDOT:PSS, where the doping level of PEDOT is modulated by a gate electrode soaked in an electrolyte.[28] We achieved OECTs by patterning multiplexed a-PEDOT:PSS gate adjacent to the a-PEDOT:PSS channel, shown schematically in Figure 4E and in micrograph Figures 4F. Using patterned PEDOT, we fabricated four transistor gates next to four independent channels. The distance between the gate and the channel was ~2 mm, and the channel length was ~1 mm. In this design, the gates shared a common contact, where they were transferred onto the device layer after assembling the device. It is also possible to pattern the channels and gates first on the same layer, followed by transferring CNT contacts onto the layer to complete the device. The gate and channels were connected by drop-casting 1 M NaCl electrolyte onto them. Figure 4G shows the performance of a representative channel. At -0.2 V gate voltage, the a-PEDOT:PSS channel oxidized (doped) and showed a high current of over -0.2 mA at -0.6 V drain-to-source voltage (VDS). The drain-to-source current (IDS) dropped as the gate voltage moved to the positive region, due to the reduction (dedoping) of

View Article Online
DOI: 10.1039/D1TC03599A

a-PEDOT:PSS channel. At around 0.5 V of gate voltage, the channel turned off, with an on/off ratio of around 20 (Figure 4H). The relatively large channel thickness and dimension, the low conductivity of CNT contacts as compared to the commonly used gold contacts, and the electrochemical oxidation at the channel at higher VDS, contribute to the lowering the on/off ratio compared to state of the art OECTs,[2] but still suffice especially for biological applications where transconductance is more important than on/off ratio. The methanol treated a-PEDOT:PSS OECT devices also showed high stability in aqueous electrolyte. We cycled the device with a switching on/off time was around ~1 s, and after 300 cycles the device retained 90% of its initial IDS as seen in Figure 4I, 4J.

We also fabricated three and four-layer devices by sandwiching the electrolyte between the OECT and the gate. First we patterned CNT finger electrodes with a distance of ~500 μm as channel length onto PEDOT:PSS cross pattern. We used a polymer membrane, poly(acrylic acid)/poly(ethylene oxide) (PAA/PEO) as a solid electrolyte. In its dry state, PAA/PEO is a free-standing, transparent membrane that can be directly superimposed onto the methanol treaded a-PEDOT:PSS/ CNT pattern, as shown schematically in Figure 4K. The mechanical properties of PAA/PEO allowed for the a-PEDOT:PSS gate layer to be pasted from the filter membrane onto the PAA/PEO membrane(Figure 4L and 4M). We showed that upon hydration of the PAA/PEO separator/electrolyte membrane, the OECT could be modulated with the a-PEDOT:PSS gate (Figure 4N,4O).

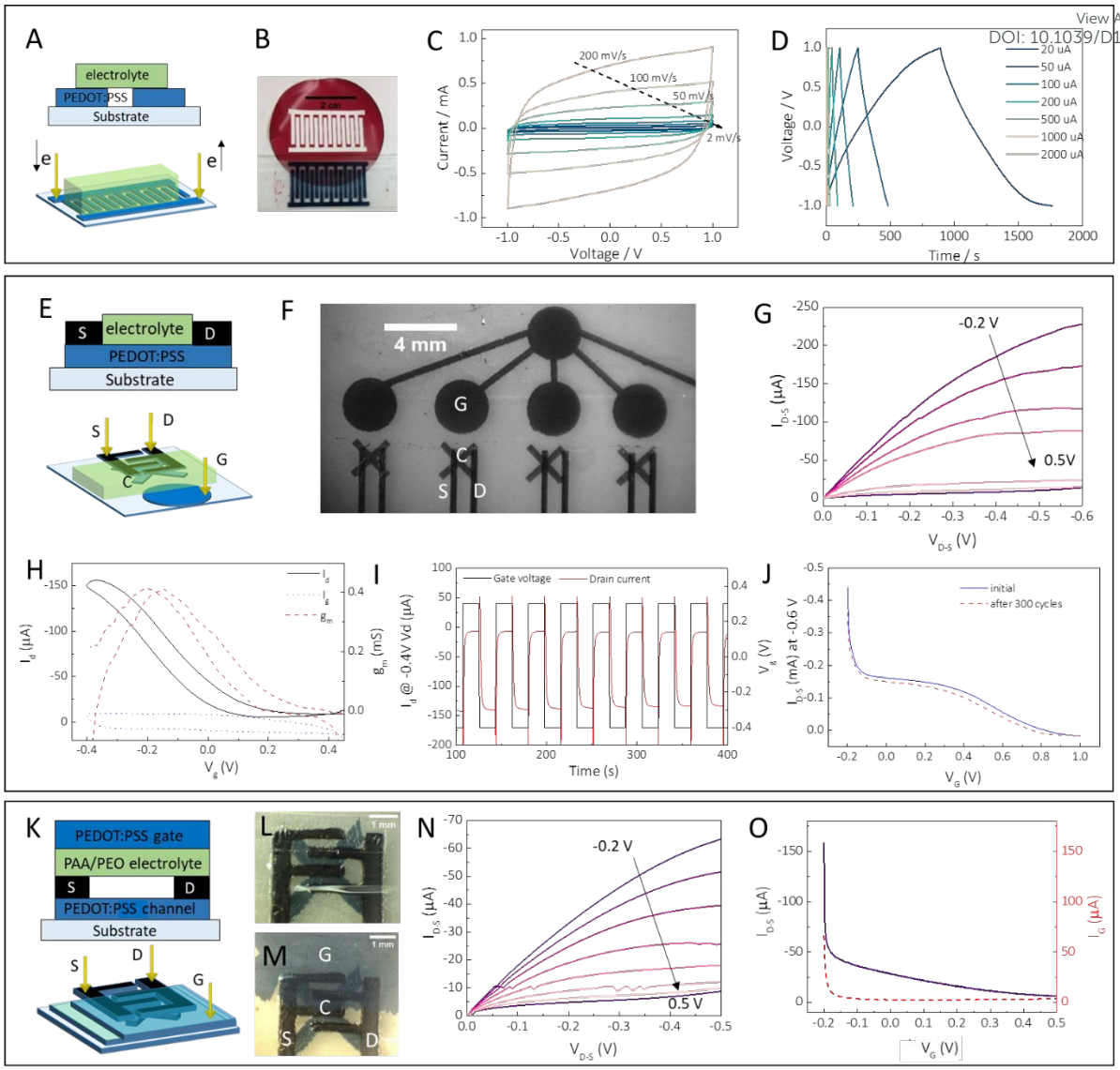

Figure 4 Heterostructures of methanol treaded a-PEDOT:PSS devices. (A) Two-layer structure of interdigitated supercapacitor. (B) Photograph of the wax patterned filtration membrane and the transferred a-PEDOT:PSS supercapacitor. (C) CVs of the device as shown in B at different scan rates. The electrolyte was 1 M NaCl. (D) Charge-discharge curve of device B. (E) Schematic of three-layer structure transistors indicating source S, drain D, channel C and gate G. (F) a-PEDOT:PSS transistor array with a multiplexed electrode. The image shows 4 channels. (G) Steady-state parameter of a transistor shown in (F). The electrolyte was PBS in agarose gel. (H) Transfer curve at VDS = -0.4 V of an a-PEDOT:PSS device showing hysteresis during sweeping. (I) Switching profile of the device in (F). The drain voltage was set at -0.4 V and the gate voltage was switched between -0.4 V and +0.3 V.

View Article Online
DOI: 10.1039/D1TC03599A

(J) Transfer curve of the device before and after 300 cycles of switching at VDS = -0.6V. (K) Schematics of four-layer structure of an a-PEDOT:PSS transistor, with the gate layer placed vertically to the channel, separated by an electrolyte membrane. (L) Optical micrograph of a transistor with an electrolyte membrane directly placed on top. (M) Optical micrograph of the same device in (L), with a-PEDOT:PSS gate transferred on top of the separator membrane. (N) Steady state parameter of the Device in M. (O) Transfer curve of the device at VDS = -0.4 V. The dotted line is the gate current. The electrolyte is 1 M NaCl.

2.6. Biocompatibility

An important application area for advanced organic electronic devices is in the field of bioelectronics in vivo and in vitro. To demonstrate that our devices were biocompatible, we used human tumor derived glioblastoma U87 cells as well as Lund Human Mescencephalic (LUHMES) neuronal cells, and cultivated them onto micropatterned methanol treaded a-PEDOT:PSS electrodes, similar to the pattern shown in Figure 2C (right). These micropatterned a-PEDOT:PSS films were transferred onto a medical tape, treated with methanol and enclosed in a Polydimethylsiloxane (PDMS) well for seeding the cells (**Figure 5A**). Medical tape was used as a substrate when involving cell cultivation due to its reported compatibility with other cell culture models and minimal cytotoxic compound compared to conventional scotch tape.[29]

We grew U87 and LUHMES cells on top of a-PEDOT:PSS electrodes as well as the tape (Figure 5C-F and Figure S5). Cell counting showed that the U87 cells continued to proliferate as their number increased compared to the seeded density of 20,000 cells per cm^2 (Figure 5G). The U87 cells proliferate at a similar rate on a-PEDOT:PSS and on the tape between two electrodes in comparison to cells growing in conventional well plates or on tape without patterned a-PEDOT:PSS electrodes. Similar cell behavior on the different surfaces was also observed when comparing the total surface area covered by U87 cells (Figure 5H).

View Article Online
DOI: 10.1039/D1TC03599A

The average areal a single cell covers on a-PEDOT:PSS and on tape was slightly lower than that observed in a conventional well plate (Figure 5I). We hypothesize that this is due to the difference in surface roughness as well as softness of PEDOT:PSS and the tape compared to the well plates made of polystyrene. The sheet resistance of the electrodes increases slightly from 21.7 ± 1.3 Ω sq^{-1} to 24.1 ± 2.5 Ω sq^{-1} after having been submerged in the cell culture media and incubated at 37 °C for two days (Figure 5B), demonstrating that the micropatterned electrodes could function in-vitro.

The analysis with the U87 cells not only shows that the cells survive on the electrodes and the medical tape, but also show similar growth behavior as in conventional cell culture well plates. This is essential when addressing biological questions for in vitro cell culture model studies. The compatibility of the described patterned a-PEDOT:PSS electrodes with U87 and LUHMES cells, gives opportunities for example for recording electrophysiological cell signals with the help of a-PEDOT:PSS based OECTs.

View Article Online
DOI: 10.1039/D1TC03599A

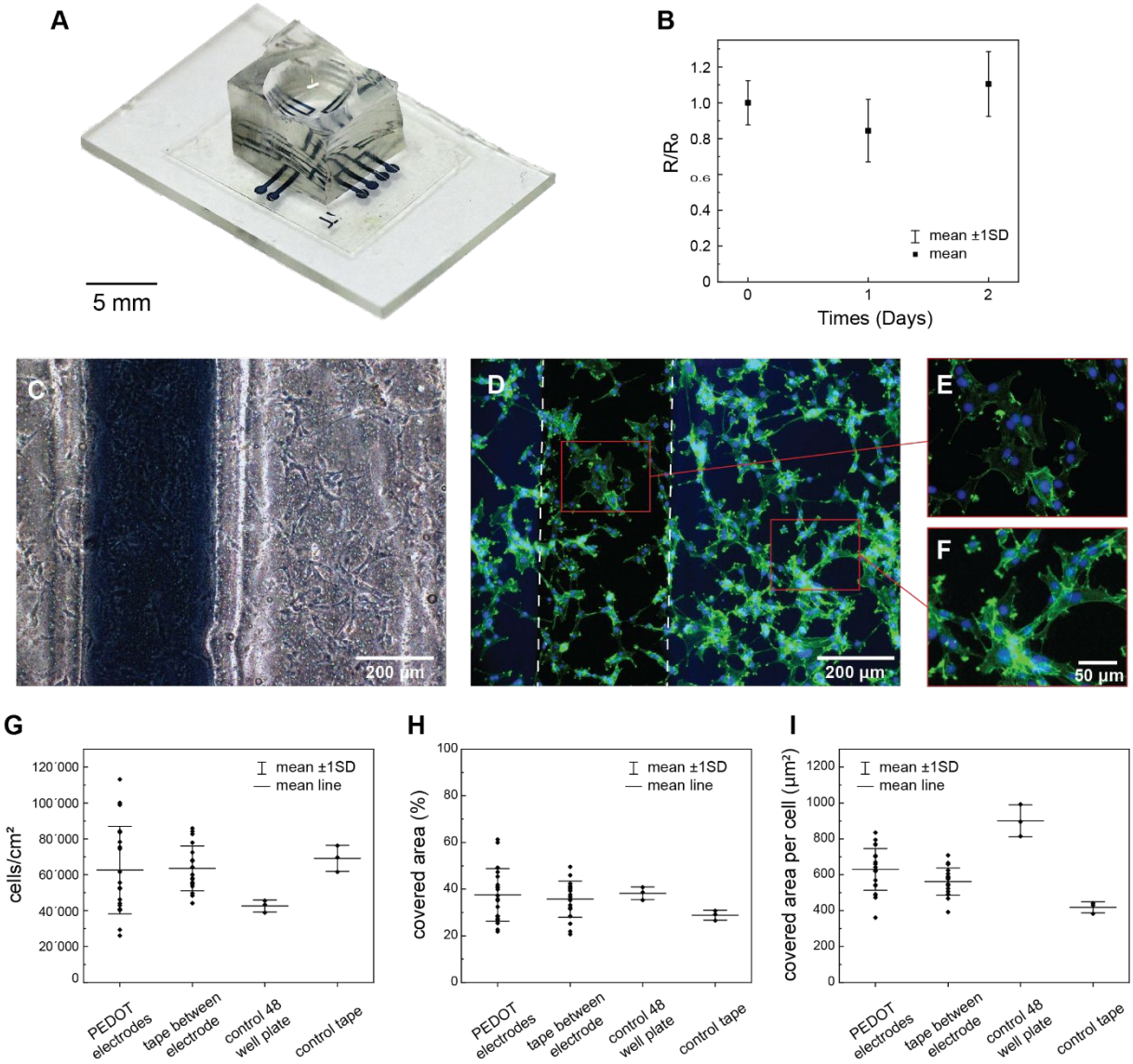

Figure 5. U87 cells cultivated for 2 days on a-PEDOT:PSS electrodes on tape. (A) Photography of the cell culture. (B) Change in resistance of the a-PEDOT:PSS micropatterns a function of time while immersed in the cell culture. (C) Brightfield image and (D) fluorescent image stained with phalloidin (green) and Hoechst (blue). (E) and (F) zoomed-in images on cells growing on a-PEDOT:PSS and tape, respectively. (G) Counted number of cells per cm^2, (H) cell coverage in percentage and (I) average cell coverage of a single cell on a-PEDOT:PSS, tape, conventional 48 well plate and on tape without patterned electrodes as control.

View Article Online
DOI: 10.1039/D1TC03599A

3. Conclusion

In conclusion, we have developed an acidified PEDOT:PSS microgel that can be facilely micro patterned with simple tools of wax printing, filtration, and adhesive tape. This method can pattern PEDOT films into arbitrary geometries with a resolution reaching 100 µm. These micropatterns have further been rendered water resilient using a post methanol treatment. Using CNTs as other types of electroactive materials dispersed in water, we could build vertically stacked, heterostructured microelectronic devices through peeling-and-pasting the different micropatterned materials. We show that this method could rapid-prototype numerous advanced microelectronic structures and devices including electrodes, micro supercapacitors and organic electrochemical transistors with up to four layers of different materials. The time and cost efficient fabrication of stable multilayer devices is a unique property of this method compared to previously described PEDOT:PSS patterning methods (see table S1). Finally, we showed that the acidified PEDOT:PSS micropatterns were compatible with human U87 and LUHMES cell cultures, which enable the use of this technique for bioelectronic devices. This method can be used with many other colloidal materials such as graphene and other 2D materials, or cellulose/protein nanofibrils, and enable rapid prototyping of a plethora of multilayer microelectronic devices and applications ranging from printed electronics,[30] to in vivo bioelectronics for drug delivery,[31] or neural contacts [24,32] and in vitro electrode interfaces for mammalian cell and bacterial cultures,[2] or for epidermal electronics**.** [33,34]

View Article Online
DOI: 10.1039/D1TC03599A

4 Materials and Methods

Material:

PEDOT:PSS (Clevios PH1000) was purchased from Heraeus. Multiwall and single wall carbon nanotube (MWCNT and SWCNT) dispersions were prepared according reference.[34] Poly(acrylic acid)/poly(ethylene oxide) (PAA/PEO) membranes were assembled by layer-by-layer assembly method according to reference.[35] Durapore PVDF (0.45 μm) membrane filters were purchased from Sigma-Aldrich. Growth factor reduced Matrigel was purchased from Corning. Advanced DMEM, N-2, l-glutamine, BSA, alexa fluor 488 phalloidin and Hoechst were purchased from Thermo Fischer. Fibroblast growth factor and GDNF were purchased from R&D Systems. Dibutyryl cAMP was purchased from Selleckchem. All the other chemicals were purchased from Sigma-Aldrich and used without purification.

Rheology measurements:

Rheology measurements of a-PEDOT:PSS hydrogels were carried out at using a DHR-2 rheometer (TA Instruments, USA) with a 25 mm diameter parallel plate geometry with a gap of 500 μm. A Peltier plate was used to keep the temperature at 25°C. The procedure was started by adding 0.3 mL PEDOT:PSS suspension with a concentration of 1.3 wt % to the Peltier plate and the top plate was lowered to the gap so that the volume between the plates were filled by the suspension. 0.3 mL sulfuric acid of different concentrations was slowly and evenly added along the circumference to initiate the gelling process, and a time sweep measurement (0.5 % strain at 1 Hz) was initiated to track the kinetics of the gelling for the first 30 minutes. The gelling was not at a steady state after 30 min, but at longer times drying of the gel was observed. The time sweep was immediately followed by a frequency (0.025% strain at 0.1 – 100 Hz) and an Amplitude sweep (0.1 -100 % strain at 1 Hz).

View Article Online
DOI: 10.1039/D1TC03599A

Preparation of acidified PEDOT:PSS (a-PEDOT:PSS):

In a vial with 10 mL PEDOT:PSS, 10 mL 1 M sulfuric acid aqueous solution was added drop wise under constant stirring. The blue precipitate was collected by centrifuging at 4500 rpm for 15 minutes. 100 mL de-ionized water was added into the pellet. The whole mixture was dispersed under vigorous stirring at 1500 rpm for overnight. The resultant dispersion of a-PEDOT:PSS was stable under room conditions. Too gentle stirring results in larger particle size of the gel dispersion and minimizes the quality and resolution of the wax printing assisted filtration.

Wax-printing assisted filtration patterning:

All the patterns were drawn by Adobe Illustrator and directly printed onto hydrophilic PVDF membranes. The membrane was hydrated before adding the materials. The stock solution of the colloids, including a-PEDOT:PSS (0.1 wt %) and CNT (1 g L^{-1}), was diluted by at least 10 times before being fileted through the membrane. The materials were retained at the hydrophilic regions of the membrane. After drying, the patterns can be either directly peeled off, transferred onto scotch tapes or on a pre-patterned tape to create heterostructure multi stack layers.

Characterizations:

Optical Image analysis was performed with Fiji. AFM images were collected under ambient conditions using a MultiMode 8 (Bruker, Santa Barbara, CA, USA) setup in SCANASYST mode with a SCANASYST-AIR cantilever.

View Article Online
DOI: 10.1039/D1TC03599A

Cell cultivation:

To cultivate cells on a-PEDOT:PSS electrodes a simple customized PDMS (Sylgard 184) based well set up was used. PDMS and curing agent were mixed at a weight ratio of 10:1, poured into a petri dish, degassed and hardened at 70 °C overnight. PDMS wells were punched out with a 6 mm biopsy-punch and placed on medical tape (3M, 9877) which had been patterned with methanol treaded a-PEDOT:PSS electrodes. Prior to cell seeding, the devices were soaked in 70% ethanol for 5 minutes, washed 3 times with PBS and coated with attachment factor protein by incubating for 30 minutes for U87 cells (ATCC) or growth factor reduced Matrigel (1:100) for LUHMES cells (abm) for 4 hours at 37 °C. U87 cells were seeded at 20'000 cells per cm^2 and cultivated in DMEM/ 10% FBS/ 1%PS for 2 days. LUHMES cells were cultivated following the protocol described by Sholz et al. [36] For proliferation cells were kept in Advanced DMEM/F12, 1x N-2 supplement, 2 mM l-glutamine ad 40 ng ml^{-1} fibroblast growth factor. Differentiation media consisted of advanced DMEM/F12, 1x N-2 supplement, 2 mM l-glutamine, 1 mM dibutyryl cAMP, 1 µg ml^{-1} tetracycline and 2 ng ml^{-1} human GDNF. To differentiate LUHMES cell were seeded into a T25 flask in proliferation media and after 24 media was changed to differentiation media for 2 days. The cells were then reseeded onto the pattered a-PEDOT:PSS electrodes at a density of 150'000 cells per cm^2. For staining, cells were fixed in 4% methanol free formaldehyde solution for 15 minutes at RT and washed 3 timed with PBS. The samples were incubated in PBS/ 0.1% Triton X-100 for 15 minutes at RT before stained with Hoechst (1:2000) in PBS for 10 minutes followed by Alexa Fluor 488 Phalloidin (1.65 µM) for 1 hour at RT and washed again 2 times with PBS. Images were acquired using a fluorescent microscope Nikon eclipse Ti-S and an Infinity 2 camera from Lumenera. Image analysis was performed using Fiji.

View Article Online
DOI: 10.1039/D1TC03599A

Author Contributions

LO and SB contributed equally to this work. LO and MH devised this project and wrote the manuscript. LO performed the experiments. CM measured the OECT performances. ZH prepared electrolytes and membranes. SB and AH performed biological tests and edited the manuscript with LO and MH. WT facilitated the filtration process. HL conducted the AFM measurements. T.B. performed the rheology measurement and analysis. All the authors have contributed to manuscript writing. The manuscript was written through contributions of all authors. All authors have given approval to the final version of the manuscript.

Conflict of Interest

The authors declare no conflict of interest.

Acknowledgments

M.M.H and L.O. acknowledge the European Research Council (Grant 715268), Z.W acknowledges the Wenner-Gren Foundation, S.B acknowledges Vetenskapsrådet, W.T. and A.H. acknowledge the Wallenberg foundation.

References

1. C. Müller, L. Ouyang, A. Lund, K. Moth‐Poulsen and M. M. Hamedi, *Advanced Materials*, 2019, **31**, 1807286.
2. E. Zeglio, A. L. Rutz, T. E. Winkler, G. G. Malliaras and A. Herland, *Advanced Materials*, 2019, **31**, 1806712.
3. S. Middya, V. F. Curto, A. Fernández‐Villegas, M. Robbins, J. Gurke, E. J. Moonen, G. S. Kaminski Schierle and G. G. Malliaras, *Advanced Science*, 2021, 2004434.
4. L. D. Garma, L. M. Ferrari, P. Scognamiglio, F. Greco and F. Santoro, *Lab on a Chip*, 2019, **19**, 3776-3786.
5. S. K. Sinha, Y. Noh, N. Reljin, G. M. Treich, S. Hajeb-Mohammadalipour, Y. Guo, K. H. Chon and G. A. Sotzing, *ACS applied materials & interfaces*, 2017, **9**, 37524-37528.
6. H. Yuk, B. Lu, S. Lin, K. Qu, J. Xu, J. Luo and X. Zhao, *Nature Communications*, 2020, **11**, 1604.
7. M. M. Hamedi, A. Ainla, F. Güder, D. C. Christodouleas, M. T. Fernández‐Abedul and G. M. Whitesides, *Advanced Materials*, 2016, **28**, 5054-5063.

8. W. Tian, A. VahidMohammadi, M. S. Reid, Z. Wang, L. Ouyang, J. Erlandsson, T. Pettersson, L. Wågberg, M. Beidaghi and M. M. Hamedi, *Advanced Materials*, 2019, **31**, 1902977.
9. K. Tybrandt and J. Vörös, *Small*, 2016, **12**, 180-184.
10. K. Tybrandt, D. Khodagholy, B. Dielacher, F. Stauffer, A. F. Renz, G. Buzsáki and J. Vörös, *Advanced Materials*, 2018, **30**, 1706520.
11. A. Hajian, Z. Wang, L. A. Berglund and M. M. Hamedi, *Advanced Electronic Materials*, 2019, **5**, 1800924.
12. S.-M. Kim, N. Kim, Y. Kim, M.-S. Baik, M. Yoo, D. Kim, W.-J. Lee, D.-H. Kang, S. Kim, K. Lee and M.-H. Yoon, *NPG Asia Materials*, 2018, **10**, 255-265.
13. G. Dijk, A. L. Rutz and G. G. Malliaras, *Advanced Materials Technologies*, 2020, **5**, 1900662.
14. O. Bubnova, Z. U. Khan, A. Malti, S. Braun, M. Fahlman, M. Berggren and X. Crispin, *Nat Mater*, 2011, **10**, 429-433.
15. W. Lövenich, *Polymer Science Series C*, 2014, **56**, 135-143.
16. S. Kim, B. Sanyoto, W.-T. Park, S. Kim, S. Mandal, J.-C. Lim, Y.-Y. Noh and J.-H. Kim, *Advanced Materials*, 2016, **28**, 10149-10154.
17. V. R. Feig, H. Tran, M. Lee, K. Liu, Z. Huang, L. Beker, D. G. Mackanic and Z. Bao, *Advanced Materials*, 2019, **31**, 1902869.
18. B. Lu, H. Yuk, S. Lin, N. Jian, K. Qu, J. Xu and X. Zhao, *Nature communications*, 2019, **10**, 1-10.
19. J. Edberg, D. Iandolo, R. Brooke, X. Liu, C. Musumeci, J. W. Andreasen, D. T. Simon, D. Evans, I. Engquist and M. Berggren, *Advanced Functional Materials*, 2016, **26**, 6950-6960.
20. S. Ghosh and O. Inganäs, *Advanced Materials*, 1999, **11**, 1214-1218.
21. Z. Li, H. Sun, C.-L. Hsiao, Y. Yao, Y. Xiao, M. Shahi, Y. Jin, A. Cruce, X. Liu, Y. Jiang, W. Meng, F. Qin, T. Ederth, S. Fabiano, W. M. Chen, X. Lu, J. Birch, J. W. Brill, Y. Zhou, X. Crispin and F. Zhang, *Advanced Electronic Materials*, 2018, **4**, 1700496.
22. L. Ouyang, C. Musumeci, M. J. Jafari, T. Ederth and O. Inganäs, *ACS applied materials & interfaces*, 2015, **7**, 19764-19773.
23. D. Alemu, H.-Y. Wei, K.-C. Ho and C.-W. Chu, *Energy & Environmental Science*, 2012, **5**, 9662-9671.
24. D. Gao, K. Parida and P. S. Lee, *Advanced Functional Materials*, 2019, 1907184.
25. K. Wijeratne, U. Ail, R. Brooke, M. Vagin, X. Liu, M. Fahlman and X. Crispin, *Proceedings of the National Academy of Sciences*, 2018, **115**, 11899-11904.
26. X. Cui and D. C. Martin, *Sensors and Actuators B: Chemical*, 2003, **89**, 92-102.
27. A. V. Volkov, K. Wijeratne, E. Mitraka, U. Ail, D. Zhao, K. Tybrandt, J. W. Andreasen, M. Berggren, X. Crispin and I. V. Zozoulenko, *Advanced Functional Materials*, 2017, **27**, 1700329.
28. J. Rivnay, S. Inal, A. Salleo, R. M. Owens, M. Berggren and G. G. Malliaras, *Nature Reviews Materials*, 2018, **3**, 1-14.
29. T. E. Winkler, M. Feil, E. F. Stronkman, I. Matthiesen and A. Herland, *Lab on a Chip*, 2020, **20**, 1212-1226.
30. H. Li and J. Liang, *Advanced Materials*, 2019, 1805864.
31. M. R. Abidian and D. C. Martin, *Biomedical Applications of Electroactive Polymer Actuators*, 2009, 279.
32. R. Green and M. R. Abidian, *Advanced Materials*, 2015, **27**, 7620-7637.
33. D.-H. Kim, N. Lu, R. Ma, Y.-S. Kim, R.-H. Kim, S. Wang, J. Wu, S. M. Won, H. Tao and A. Islam, *science*, 2011, **333**, 838-843.

34. Z. Wang, L. Ouyang, W. Tian, J. Erlandsson, A. Marais, K. Tybrandt, L. Wågberg and M. M. Hamedi, *Langmuir*, 2019, **35**, 10367-10373.
35. Z. Wang, L. Ouyang, H. Li, L. Wågberg and M. M. Hamedi, *Small*, 2021, **17**, 2100954.
36. D. Scholz, D. Pöltl, A. Genewsky, M. Weng, T. Waldmann, S. Schildknecht and M. Leist, *Journal of neurochemistry*, 2011, **119**, 957-971.